# Theoretical Investigation of the Low-Lying Electronic States of Dioxirane: Ring Opening to Dioxymethane and Dissociation into $CO_2$ and $H_2$

**Josep M. Anglada,*,†,‡ Josep M. Bofill,§ Santiago Olivella,*,†,§,⊥ and Albert Solé[||]**

*Centre d'Investigació i Desenvolupament del CSIC, Jordi Girona 18, 08034-Barcelona, Catalunya, Spain, and Departaments de Quimica Orgànica i Quimica Fisica, Universitat de Barcelona, Martí i Franquès 1, 08028-Barcelona, Catalunya, Spain*

*Received: December 11, 1997; In Final Form: February 27, 1998*

The low-lying electronic states of dioxirane (**1**), their ring opening to dioxymethane (**2**), and the dissociation of **2** into $CO_2$ and $H_2$ have been investigated by means of CASSCF and MRD-CI+Q quantum chemistry calculations. The ground state of **1** is a singlet with $4\pi$ electrons, $1^1A_1(4\pi)$, while the ground state of **2** is a $2\pi$-electron singlet, $1^1A_1(2\pi)$, lying 5.8 kcal/mol higher than **1** in energy. A 0 K activation energy of 21.4 kcal/mol is predicted for the thermal ring opening of **1** into **2**, which takes place via a transition structure approximately corresponding to the crossing between the lower $^1A_1(4\pi)$ and $^1A_1(2\pi)$ states of both molecules. Twelve excited states have been calculated for **1** with vertical excitation energies ranging from 3.07 to 13.11 eV. The energy ordering of these states changes dramatically upon relaxation of the molecular geometries. The optimum geometries of these excited states show an ∠OCO in the 106.3−120.1° range, so they should be considered as excited states of **2**. Minimum energy points of the intersection seam between the $1^1A_2$-$(3\pi)/1^1B_1(3\pi)$, $1^1B_1(3\pi)/^1A_1(2\pi)$, $1^1A_2(3\pi)/^1A_1(4\pi)$, and $1^1B_1(3\pi)/^1A_1(4\pi)$ potential energy surfaces have been located in an ∠OCO range of 91.0−104.6°. The photochemical ring opening of **1** into **2** may occur through vertical excitation to either the $1^1B_1(3\pi)$ or $1^1A_2(3\pi)$ states of **1** and subsequent radiationless decay to ground-state **2** via minimum energy intersection points on the potential energy surfaces of the appropriate states. The dissociation of ground-state **2** into $CO_2$ and $H_2$ is predicted to be exothermic by 105.2 kcal/mol with a 0 K activation energy of 3.2 kcal/mol, while the dissociations of the first four excited states of **2** are all predicted to be endothermic.

## 1. Introduction

Dioxiranes represent the class of the most strained cyclic organic peroxides, containing one carbon and two oxygen atoms in a three-membered ring. They can be formed by thermal or photochemical isomerization of carbonyl oxides during the ozonolysis of alkenes or the oxidation of carbenes.[1,2] In 1977, the parent dioxirane molecule **1** was identified by microwave spectroscopy[3] and was also detected by mass spectroscopy[4] in the gas phase as an intermediate in the low-temperature reaction between ozone and ethylene. To date only a few dioxiranes appear to have been isolated as relatively stable compounds.[5] The involvement of dioxiranes and their isomeric counterparts carbonyl oxides as short-lived reaction intermediates has been postulated in many oxidation reactions (e.g., ozonolysis, Baeyer−Villiger reaction)[6−8] and enzymatic processes.[9] Furthermore, dioxiranes are currently of interest because of their importance in the chemistry of urban air pollution[10] and as effective oxygen carriers for regio- and stereoselective epoxidations.[11]

In a seminal theoretical study on the mechanism of olefin ozonolysis Wadt and Goddard[12a] found that generalized valence bond (GVB) calculations described the ground state of **1** as singlet ($^1A_1$ in $C_{2v}$ molecular symmetry) that has the $\pi$-type atomic 2p orbitals on both oxygen atoms doubly occupied.

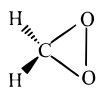

**1**

**2**

Following Goddard's nomenclature, this structure is referred to as the $^1A_1(4\pi)$ state of **1**, and the electron occupation of the oxygen 2p orbitals can be depicted by the following diagrams:

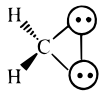

$^1A_1(4\pi)$

Here, each oxygen 2p orbital perpendicular to the plane of the paper is represented by a circle and dots indicate the number of electrons in each orbital. The weakest bond in **1** is the peroxide bond, which has an estimated OO bond dissociation energy of about 36 kcal/mol.[13] It was suggested that methylenebis(oxy) ("dioxymethane") (**2**), resulting from homolytic OO bond cleavage of **1**, could make a contribution to the chemistry of dioxirane.[12a] The ground state of **2** was found to be a singlet diradical of $A_1$ symmetry that has the $\pi$-type atomic 2p orbitals on both oxygen atoms singly occupied with the two oxigen lone pairs in the OCO plane. GVB configuration interaction (GVB-CI) calculations by Harding and Goddard[12b] predicted this diradical structure, referred to as the $^1A_1(2\pi)$ state of **2**, to be 0.48 eV more energetic than ground-state **1**. The lowest excited

† Centre d'Investigació i Desenvolupament del CSIC.
‡ E-mail: anglada@qteor.cid.csic.es.
§ Departament de Química Orgànica, Universitat de Barcelona.
⊥ E-mail: olivella@taga.qo.ub.es.
|| Departament de Química Física, Universitat de Barcelona.

S1089-5639(98)00501-5 CCC: $15.00 
Published on Web 04/22/1998

state of **2** was found to be the $2\pi$-electron triplet state of $B_2$ symmetry, referred to as the $^3B_2(2\pi)$ state of **2**, originating from the latter diradical electron configuration by triplet spin coupling of the two unpaired electrons.

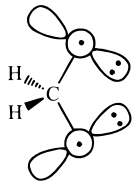

$^1A_1(2\pi)$, $^3B_2(2\pi)$

At the GVB-CI level this $^3B_2$ state lies only 0.04 eV above the ground state of **2**.[12b] In addition, two singlet and two triplet states of $A_2$ and $B_1$ symmetry, arising from the $3\pi$-electron configuration of **2**, were found to be 0.12−0.66 eV above its ground state.[12b]

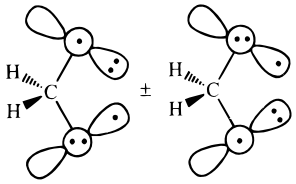

$^{1,3}A_2(3\pi)$, $^{1,3}B_1(3\pi)$

The singlet $^1A_1(4\pi)$ state of **2** with the two $\pi$-type atomic 2p orbitals on both oxygen atom doubly occupied and two oxygen singly occupied atomic 2p orbitals in the plane of the ring was calculated to lie 0.49 eV above the ground-state $^1A_1(2\pi)$.[12b] Finally, the $^3B_2$ state arising from the latter electron configuration by triplet spin coupling of the two unpaired electrons was located 0.56 eV above the ground state of **2**.[12b]

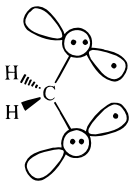

$^1A_1(4\pi)$, $^3B_2(4\pi)$

It should be pointed out that all these GVB-CI calculations were performed at the equilibrium geometry assumed for the ground state of **2**. Later multiconfiguration self-consistent field (MCSCF) calculations by Karlström and co-workers[14] predicted the ground states of **1** and **2** to have almost the same energy, **1** being 0.07 eV more stable. The adiabatic energy barrier for the ring opening of **1** to **2** was calculated to be 0.66 eV. More recently Bach and co-workers[15] have studied the structure and relative energy of **1** and **2** at a variety of levels including complete active space self-consistent field (CASSCF), second- and fourth-order Moller−Pleset perturbation theory (MP2 and MP4), and quadratic configuration interaction with singles, doubles, and perturbative estimation of triples method (QCISD(T)). Their best calculation of the **1**/**2** relative energy was 12.4 kcal/mol (0.54 eV) and was obtained from QCISD(T)/6-31G(d) energies computed at the QCISD/6-31G(d) optimized geometries. The geometries of two excited states of **2**, corresponding to $3\pi$- and a $4\pi$-electron singlets, were optimized at the MP2/6-31G(d) level. Single-point QCISD(T)/6-31G(d) calculations located these excited states 0.50 and 1.15 eV, respectively, above the ground state. Quite recently, Cantos and co-workers[16] have reported a theoretical study of the geometry and electronic spectra of **1**, **2**, and its anion using CASSCF and second-order perturbation theory (CASPT2). the ground state of **2** was located 0.48 eV above **1**, and an energy barrier of 1.12 eV was calculated for the ground-state isomerization of **1** to **2**. The first vertical excitation energy of **1** was found to be 4.1 eV and to correspond to a $3\pi$-electron singlet of $B_1$ symmetry. No other vertical excitations of **1** were calculated in the theoretical study of Cantos and co-workers. For **2** seven vertical excited states were located below 2 eV. The adiabatic excited states of **1** or **2** were, however, not included in that theoretical study.

We feel that the excited states of **1** and **2** merit further study. It is the purpose of this paper to examine with accurate *ab initio* calculations the electronic structure and relative energies of the low-lying electronic states of **1** and their ring opening to **2**. It is our goal to shed light on the implication of these states on the thermal and photochemical fate of the dioxiranes produced in the low-temperature gas-phase reaction between ozone and olefins. In addition, since carbon dioxide is one of the major reaction products formed in the latter reaction,[17] the dissociation of the low-lying electronic states of **2** into $CO_2$ and $H_2$ has also been investigated by means of accurate *ab initio* calculations.

## II. Electronic Structure Considersiderations

Previous studies on **1** have shown that at all levels of theory its electronic ground state is a closed-shell singlet with $4\pi$ electrons which has $C_{2v}$ molecular symmetry.[18] Considering only the valence electrons of the CO and OO bonds and the out of plane lone-pair electrons of the oxygen atoms, the ground state of **1**, denoted $1^1A_1$, can be quantitatively described by the electronic configuration

$$... 5a_1^2\, 6a_1^2\, 3b_2^2\, 2b_1^2\, 1a_2^2 \qquad (1)$$

Essentially, the $5a_1$ and $3b_2$ molecular orbitals (MOs) correspond to the symmetric and antisymmetric combinations, respectively, of the two CO $\sigma$-bonds, whereas $6a_1$ describes the OO $\sigma$-bond. The $2b_1$ and $1a_2$ MOs are $\pi$-type orbitals corresponding to the symmetric and antisymmetric combinations, respectively, of the out of plane p nonbonding orbitals of the oxygen atoms. The ground state of **1** therefore has $4\pi$ electrons.

At the self-consistent-field (SCF) level of theory, the lowest unoccupied MO is the $4b_2$ orbital, which corresponds to the OO $\sigma^*$-bond. The low-lying excited states of **1** arise from single and double excitations from the three highest occupied orbitals, namely $6a_1$, $2b_1$, and $1a_2$, to the unoccupied $4b_2$ orbital. Thus, single excitation (relative to configuration eq 1) from the $1a_2$ orbital to the $4b_2$ orbital yields an open-shell electronic configuration with $3\pi$ electrons, which can be written in short form as

$$... 5a_1^2\, 6a_1^2\, 3b_2^2\, 2b_1^2\, 1a_2^1\, 4b_2^1 \qquad (2)$$

This configuration gives rise to one singlet and one triplet states of $B_1$ symmetry. Single excitation (relative to configuration eq 1) from the $2b_1$ orbital to the $4b_2$ orbital yields another open-shell electronic configuration, which can be written as

$$... 5a_1^2\, 6a_1^2\, 3b_2^2\, 2b_1^1\, 1a_2^2\, 4b_2^1 \qquad (3)$$

This configuration gives rise to one singlet and one triplet states of $A_2$ symmetry with $3\pi$ electrons.

The low-lying electronic states of $B_2$ symmetry, namely the open-shell states $^3B_2$ and $^1B_2$, may arise from the electronic

configuration obtained from single excitation (relative to configuration eq 1) from the $6a_1$ orbital to the $4b_2$ orbital that can be written as

$$... 5a_1^2\, 6a_1^2\, 3b_2^2\, 2b_1^2\, 1a_2^2\, 4b_2^1 \quad (4)$$

This configuration has $4\pi$ electrons. Regarding possible low-lying excited states of **1** generated from double excitations relative to configuration eq 1, it will be shown below that there is another $^3B_2$ state with $2\pi$ electrons, which arises from the electronic configuration

$$... 5a_1^2\, 6a_1^2\, 3b_2^2\, 2b_1^1\, 1a_2^1\, 4b_2^2 \quad (5)$$

Finally, double excitation (relative to configuration eq 1) from either the $1a_2$ or $2b_1$ orbitals to the $4b_2$ orbital gives rise to closed-shell electronic configurations with $2\pi$ electrons, which can be written as

$$... 5a_1^2\, 6a_1^2\, 3b_2^2\, 2b_1^2\, 4b_2^2 \quad (6)$$

$$... 5a_1^2\, 6a_1^2\, 3b_2^2\, 1a_2^2\, 4b_2^2 \quad (7)$$

The combination of configurations eqs 6 and 7 leads to a $2\pi$-electron singlet state of $A_1$ symmetry, denoted $2^1A_1$. As mentioned above, the $4b_2$ orbital is OO antibonding; therefore, one would expect the optimum molecular geometries of the states in which this orbital is singly (i.e., $^{1,3}B_1$, $^{1,3}B_2$, $^{1,3}A_2$) or doubly (i.e., $2^1A_1$) occupied to show a wider OCO bond angle, as compared with the geometry of the ground state $^1A_1$.

As noted in section I, earlier studies on **2** indicate that its ground state shows $C_{2v}$ symmetry, has $2\pi$ electrons, and possesses singlet diradical character.[12,14−16] The relevant valence MOs of **2** are the orbitals described above for **1**, except that now the $6a_1$ and $4b_2$ MOs correspond to the symmetric and antisymmetric combinations, respectively, of the in-plane p nonbonding orbitals of the oxygen atoms. The wave function for the ground state of **2** ($^1A_1$) is obtained as a combination of two nearly degenerate closed-shell configurations which are just the doubly excited configurations eqs 6 and 7 of **1**.[14,16] Therefore, the ground state of **2** correlates with the doubly-excited state $2^1A_1$ of **1**. On the other hand, **2** has a low-lying doubly excited singlet state of $A_1$ symmetry with $4\pi$ electrons whose wave function is obtained as a combination of configuration eq 1 with another closed-shell configuration which can be written in short form as

$$... 5a_1^2\, 3b_2^2\, 1a_2^2\, 2b_1^2\, 4b_2^2 \quad (8)$$

Therefore, this doubly excited state of **2** correlates with the electronic ground state of **1**. As shown by Cimiraglia and coworkers,[19] it turns out that the ground-state symmetric ring opening of **1** yielding the ground state of **2** involves a crossing of the $1^1A_1$ and $2^1A_1$ adiabatic potential energy surfaces (PESs) of these species.

### III. Methods and Computational Details

The *ab initio* MRD-CI (multireference single and double-excitation configuration interaction) method with configuration selection, energy extrapolation, and full CI estimate was employed for the calculation of the various low-lying electronic states of **1** and **2**, using the program package of Buenker and Peyerimhoff.[20] In this procedure the reference set consists of all configurations which appear in the final CI expansion with a coefficient of roughly $c^2 \geq 0.02$. The SCF MOs for the respective states are employed to construct the configurations; all nonvalence MOs are frozen. Configuration selection is undertaken at a threshold $T$ in a standard manner[20a] and the resulting secular equation solved directly. Next, the first-order density matrix corresponding to this MRD-CI calculation employing SCF MOs is simply diagonalized for obtaining the natural orbitals, which are subsequently employed in a final MRD-CI calculation. The effect of the remaining configurations of the total MRD-CI space on the energy of the system is accounted for by a self-correcting perturbation-type (extrapolation) procedure.[20b,c] Finally, the energy corresponding to the full CI space of the given basis set, designated $E$(MRD-CI+Q), is estimated in analogy to the formula given by Langhoff and Davidson[21] as

$$E(\text{MRD-CI+Q}) = E(\text{MRD-CI}) + (1 - \sum c_0^2)(E(\text{MRD-CI}) - E(\text{ref})) \quad (9)$$

where the sum is taken over all spin-adapted configuration state functions in the reference set and $E$(MRD-CI) and $E$(ref) are the total energies of the MRD-CI and reference set wave functions.[22]

Two basis sets have been used in this study. The basis set designated BS1 is the split-valence d-polarized 6-31G(d) basis,[23] consisting of 49 contracted Gaussian functions for the $CH_2O_2$ system. The other basis set, designated BS2, is the standard Huzinaga−Dunning double-$\zeta$ basis (9s5p/4s2p) contractions for C and O, (4s/2s) for H,[24,25] augmented by a diffuse p-type function on C and O (orbital exponents $\alpha_p(C) = 0.034$ [26] and $\alpha_p(O) = 0.05$ [27]), two d-type polarization functions on C and O (orbital exponents $\alpha_d(C) = 1.097$ and 0.318, and $\alpha_d(O) = 2.314$ and 0.645 [28]), and a p-type polarization function on H (orbital exponent $\alpha_p(H) = 1.0$[29]). For the $CH_2O_2$ system, BS2 consist of 85 contracted Gaussian functions. Such a basis set was chosen to reproduce accurately the adiabatic excitation energies of carbon dioxide, since it will be shown below that several low-lying electronic states of **1** and **2** dissociates into various excited states of this molecule. The adiabatic excitation energies of the four lower excited electronic states of $CO_2$ calculated at the MRD-CI+Q level of theory using the BS1 and BS2 bases are compared in Table 1 with those computed by the internally contracted multireference configuration interaction (MRCI) method with a more flexible basis set and known experimental data.[30] It is to be noted that the excitation energies computed with BS2 are reasonably close to experiment, whereas those computed with the BS1 basis deviate by about 0.3 eV.

The molecular geometries of the stationary points were optimized at the MRD-CI level by employing numerically

**TABLE 1: Geometrical Parameters[a] and Relative Energies (eV) of the Low-Lying Electronic States of Carbon Dioxide**

| | geometry | | relative energy | | | |
|---|---|---|---|---|---|---|
| | | | MRD-CI+Q[b] | | | |
| state | $R$(CO) | ∠OCO | BS1 basis | BS2 basis | MRCI[c] | expt[d] |
| $^1\Sigma_g+$ | 1.162 | 180.0 | 0.00 | 0.00 | 0.00 | 0.00 |
| $^3B_2$ | 1.251 | 118.5 | 4.51 | 4.84 | 4.75 | ≤4.88 |
| $^3A_2$ | 1.261 | 127.4 | 5.15 | 5.40 | 5.42 | |
| $^1A_2$ | 1.262 | 127.0 | 5.29 | 5.63 | 5.61 | ≤6.2−7.2 |
| $^1B_2$ | 1.260 | 117.8 | 5.46 | 5.77 | 5.74 | ≈5.7 |

[a] Optimized at the MRD-CI/BS1 level. Distances are in angstroms; angles, in deg. [b] All energies relative to the energy of the electronic ground state ($^1\Sigma_g^+$): $E$(MRD-CI+Q/BS1) = −188.10950 hartree and $E$(MRD-CI+Q/BS2) = −188.19734 hartree. [c] Internally contracted multireference configuration interaction calculations from ref 30. [d] Energy regions in which bent states of $CO_2$ have been detected. See ref 30.

**TABLE 2: Geometrical Parameters,[a] Electric Dipole Moments ($\mu$, D),[b] Zero-Point Vibrational Energies (ZPVE, kcal/mol),[c] Total Energies (E, hartree),[d] and Relative Energies ($E_{rel}$, kcal/mol),[d,e] Calculated for Dioxirane (1), Dioxymethane (2), and the Transition Structure (TS1) for the Ring Opening of Ground-State 1 into 2**

| structure | *R*(CO) | *R*(OO) | *R*(CH) | ∠OCO | ∠HCH | $\mu$ | ZPVE | *E* | $E_{rel}$ |
|---|---|---|---|---|---|---|---|---|---|
| **1** | 1.384 (1.386) | 1.512 (1.508) | 1.086 (1.083) | 66.2 (65.9) | 116.4 (116.3) | 2.67 | 19.6 | −189.215 41 | 0.0 |
| **TS1** | 1.377 | 2.108 | 1.086 | 99.9 | 110.7 | 2.55 | 18.4 | −189.179 36 | 22.6 (21.4) |
| **2** | 1.361 (1.363) | 2.359 (2.356) | 1.101 (1.099) | 120.1 (119.6) | 107.4 (107.7) | 2.12 | 18.3 | −189.204 10 | 7.1 (5.8) |

[a] Optimized at the MRD-CI/BS1 level except **TS1**, which was optimized at the CASSCF(6,4)/BS1 level. The results in parentheses were obtained with the BS2 basis; $C_{2v}$ symmetry, with distances in angstroms and angles in deg. [b] Calculated at the MRD-CI/BS2 level of theory. [c] Obtained from CASSCF(6,4)/BS1 harmonic vibrational frequencies scaled by 0.8929. [d] MRD-CI+Q/BS2 energies at the MRD-CI/BS1 optimized geometries except for **TS1**, where the CASSCF(6,4)/basis A optimized geometry was used. [e] ZPVE corrected values are given in parentheses.

calculated gradients[31] in a recently proposed restricted quasi-Newton−Raphson procedure[32] using the BS1 basis. To establish that the optimized molecular geometries are converged with respect to the basis set, additional geometry optimizations were performed for the ground state of **1** and **2**, as well as for the first excited state ($^3B_2$) of **2**, with the BS2 basis. The MRD-CI calculations carried out with the BS1 ($T = 2$ $\mu$hartrees) and BS2 ($T = 3$ $\mu$hartrees) basis sets generated MRD-CI spaces whose size varied roughly from $6 \times 10^5$ to $22 \times 10^6$, while the size of the selected subspaces, namely the dimensions of the secular equations actually solved, was on the order 17 000−32 000.

The normal modes and harmonic vibrational frequencies of the stationary points of the lowest state of each symmetry and multiplicity were obtained by using the CASSCF method[33] with the BS1 basis by diagonalizing the mass-weighted Cartesian force constant matrix calculated analytically.[34] The zero-point vibrational energies (ZPVEs) were determined from the harmonic vibrational frequencies scaled by 0.8929 (the reciprocal of 1.12).[35] The CASSCF wave function of each electronic state was obtained by distributing six-electrons in the $6a_1$, $2b_1$, $1a_2$, and $4b_2$ MOs. As mentioned in section II, these orbitals define the smallest active space that can describe the low-lying electronic states of each symmetry and multiplicity. The CASSCF geometry optimizations and harmonic vibrational frequencies calculations were carried out by using the GAMES[36] and Gaussian 94[37] codes, respectively.

The vertical excitation energies of the low-lying excited electronic states of **1** were computed at the MRD-CI+Q level with the BS2 basis using the MRD-CI/BS1 equilibrium geometry of the ground state of **1**. The electronic transition moment of the dipole-allowed vertical transitions were evaluated by employing the length operator. Finally, the adiabatic excitation energies were determined from the MRD-CI+Q/BS2 energies of each state calculated using the molecular geometries optimized at the MRD-CI/BS1 level.

## IV. Results and Discussion

**Ground-State Ring Opening of Dioxirane.** The most relevant geometrical parameters of the MRD-CI/BS1 optimized structures for the ground state of **1** and **2** are given in Table 2, along with the calculated electric dipole moments, ZPVE, and total energies. For comparison, the geometrical parameters obtained at the same level of theory with the BS2 basis are shown in parentheses. Overall, the geometrical parameters computed with both basis sets agree closely. It is satisfying to note that the calculated geometrical parameters of **1** are in excellent agreement with the reported experimental data obtained from microwave spectroscopy (*R*(OO) = 1.516 Å, *R*(CO) = 1.388 Å, ∠OCO = 66.2°, ∠HCH = 117.3°).[3] Recently, Schaefer and co-workers[18g] have reported a theoretical study demonstrating the importance of using f-type polarization functions in the *ab initio* description of the geometry and vibrational frequences of **1**. As concerns the equilibrium geometry, the present MR-DCI calculations indicate that satisfactory results are obtained for **1** using Pople's split-valence d-polarized 6-31G(d) basis set. Furthermore, the calculated dipole moment of 2.67 D is reasonably close to the experimental value of 2.48 D.[3] Regarding **2**, the computed geometrical parameters *R*(CO) = 1.361 Å and ∠OCO = 120.1° are in fairly good agreement with the values obtained from previous calculations at the MP2 (*R*(CO) = 1.367 Å and ∠OCO = 118.5°),[15b] QCISD (*R*(CO) = 1.306 Å and ∠OCO = 129.6°),[15b] and CASPT2 (*R*(CO) = 1.321 Å and ∠OCO = 127.0°)[16] levels of theory, although the QCISD and CASPT2 calculations predict a shorter CO bond length and a wider ∠OCO. As noted in section II, the wave function for the ground state of **2** corresponds chiefly to a combination of two nearly-degenerate closed-shell configurations and it is not expected that single-configuration-based methods will be adequate in this case. It is therefore surprising the close agreement between the MRD-CI and MP2 results for ground-state **2**.

At the MRD-CI+Q/BS2 level, the ground state of **2** is calculated to lie 7.1 kcal/mol above the ground state of **1**. This energy difference compares well with the earlier value of 6.2 kcal/mol obtained from two-reference CISD calculations by Karlström and co-workers[14] but is about 4−5 kcal/mol lower than the values obtained from previous calculations at different levels of theory: 11.3 kcal/mol (PMP4),[15b] 12.5 kcal/mol (QCISD(T)),[15b] and 11.1 kcal/mol (CASPT2).[16] The ZPVE correction lowers to 5.8 kcal/mol the relative energy of **2** with respect to **1**.

The ground-state symmetric ring opening of **1** into **2** was first studied by computing the adiabatic potential energy curves (PECs) for the $1^1A_1$ and $2^1A_1$ states of these species as a function of ∠OCO. For both states ∠OCO was varied and all other parameters were optimized at each fixed value of ∠OCO keeping $C_{2v}$ symmetry. These calculations were performed at the MRD-CI level with the BS1 basis. An intersection between the two PECs was found at ∠OCO ≈ 100°. This result is in good agreement with earlier calculations at the CIPSI[19] and CASPT2[16] levels of theory which predicted a crossing between the $1^1A_1/2^1A_1$ PECs to occur at ∠OCO of 102 and 100°, respectively. The changes in the composition of the MRD-CI/BS1 wave function of the $1^1A_1$ and $2^1A_1$ states throughout the ring opening of **1**, in terms of the weight of the dominant $2\pi$- and $4\pi$-electron configurations in the CI expansion, were also studied. As expected, for ∠OCO smaller than 100° the MRD-CI wave function of $1^1A_1$ is dominated by the $4\pi$-electron configuration eq 1, while the MRD-CI wave function of $2^1A_1$ is mainly described by a combination of the $2\pi$-electron configurations eqs 6 and 7. Nearby the intersection of the two potential curves, that is at ∠OCO ≈ 100°, the composition of the two wave functions is suddenly reversed, so for ∠OCO ≥ 100° the MRD-CI wave function of $1^1A_1$ corresponds chiefly to an almost equal mixture of the $2\pi$-electron configurations

**TABLE 3: Vertical Excitation Energies ($T_V$, eV),[a] Electric Dipole Moments ($\mu$, D),[b] and Oscillator Strengths ($f$)[c] of the Low-Lying Excited States of Dioxirane**

| state | $T_V$ | $\mu$ | $f$ |
|---|---|---|---|
| $1^3B_1(3\pi)$ | 3.07 | 2.55 | |
| $1^1B_1(3\pi)$ | 4.23 | 2.57 | 0.0005 |
| $1^3A_2(3\pi)$ | 5.72 | 3.30 | |
| $1^1A_2(3\pi)$ | 6.14 | 3.38 | forbidden |
| $1^3B_2(4\pi)$ | 6.39 | 2.90 | |
| $2^1A_1(2\pi)$ | 8.44 | 2.54 | 0.005 |
| $2^3B_2(2\pi)$ | 9.91 | 2.73 | |
| $1^1B_2(4\pi)$ | 9.97 | 2.23 | 0.1 |
| $2^3B_1(3\pi)$ | 11.81 | 2.85 | |
| $2^3A_2(3\pi)$ | 11.95 | 2.93 | |
| $2^1B_1(3\pi)$ | 12.42 | 2.86 | 0.00001 |
| $2^1A_2(3\pi)$ | 13.11 | 3.09 | forbidden |

[a] Calculated at the MRD-CI+Q/BS2 level. [b] Calculated with the MRD-CI/BS2 wave function of each state using the optimized geometry of dioxirane. [c] Calculated at the MRD-CI/BS2 level.

eqs 6 and 7, whereas $2^1A_1$ is dominated by a combination of the $4\pi$-electron configurations eqs 1 and 8.

The ground-state ring opening of **1** into **2** was further investigated by employing the CASSCF(6,4) wave function described in section III with the BS1 basis. A transition structure of $C_{2v}$ symmetry, **TS1**, connecting the equilibrium structures calculated for **1** and **2** was located. The optimized geometry of **TS1** is given in Table 2, along with the calculated dipole moment, ZPVE, and total energy. The geometrical parameters found for **TS1** are in good agreement with the values ($R$(CO) = 1.382 Å, ∠OCO = 103.0°, and ∠HCH = 113.7°) of the transition structure optimized by Karlström and co-workers[14] using an MCSCF wave function consisting of 10 closed-shell determinants. It is worth noting that the geometry of **TS1** is close to the found at the MRD-CI level for the $1^1A_1$ state of **1** with ∠OCO fixed at 100°, namely $R$(CO) = 1.400 Å, $R$(CH) = 1.092 Å, and ∠HCH = 111.5°, which approximately corresponds to the structure of the intersection point between the $^1A_1(4\pi)$ and $^1A_1(2\pi)$ adiabatic PECs. Indeed, at the **TS1** geometry the MRD-CI+Q/BS2 energy of the $^1A_1(4\pi)$ state[38] is only 0.1 kcal/mol higher than that of the $^1A_1(2\pi)$ state. According to Table 2, the potential energy barrier for the ground-state ring opening of **1** to **2** is predicted to be 22.6 kcal/mol at the MRD-CI/BS2 level. This energy barrier can be compared with the earlier values of 15.2 and 25.8 kcal/mol obtained from MCSCF[14] and CASPT2[16] calculations, respectively. It should be noted the CASPT2 calculations of Cantos and co-workers were performed optimizing ∠OCO with all other parameters held fixed at their values in **1**. The ZPVE correction to the MRD-CI+Q/BS2 energy barrier leads to a 0 K activation energy of 21.4 kcal/mol.

**Low-Lying Excited Electronic States of Dioxirane and Dioxymethane.** Table 3 shows the calculated vertical excitation energies for the first 12 excited electronic states of **1**, along with the dipole moments and oscillator strengths. To characterize the electronic structure, each state is labeled according to the number of $\pi$ electrons. Detailed information about the MRD-CI/BS1 wave functions for these states is given in the penultimate column of Table 4. Summarized there are the most important configurations and their weights (in percent) in the CI expansion. As seen in Table 3, the first four vertical excited states of **1** are found to be triplet and singlet states of $B_1$ and $A_2$ symmetry. According to Table 4, the dominant configuration of these states corresponds to the singly excited configurations $1a_2 \rightarrow 4b_2$ (eq 2) and $2b_1 \rightarrow 4b_2$ (eq 3), respectively. Following the orbital energy ordering shown in section II, that is $2b_1 <$ $1a_2$, the $1^3B_1(3\pi)$ and $1^1B_1(3\pi)$ states are predicted to lie below the $1^3A_2(3\pi)$ and $1^1A_2(3\pi)$ states. The vertical excitation energy of 4.23 eV found for the first excited singlet, $1^1B_1(3\pi)$, is in agreement with the earlier value of 4.1 eV obtained from CASPT2 calculations.[16] The fifth vertical excited state of **1** is found to be the $1^3B_2(4\pi)$ state arising mainly from a mixture of the singly excited configurations $6a_1 \rightarrow 4b_2$ (eq 4) and $5a_1 \rightarrow 4b_2$. The singlet state arising from the same singly excited configurations, $1^1B_2(4\pi)$, is found to lie 3.58 eV above the $1^3B_2(4\pi)$ state. This singlet−triplet energy splitting is much larger than the calculated for the lower excited states of $B_1(3\pi)$ and $A_2(3\pi)$ symmetry, namely 1.16 and 0.42 eV, respectively. This result can be rationalized in terms of the different spatial localization of the singly occupied MOs $6a_1$, $1a_2$, and $2b_1$, which distinguish the above $B_2(4\pi)$, $B_1(3\pi)$, and $A_2(3\pi)$ states. Thus the exchange integral, causing most of the energy splitting between the singlet and triplet states originating from the same electronic configuration, is expected to be larger for the orbital pair $6a_1-4b_2$ than for either the $1a_2-4b_2$ or $2b_1-4b_2$ orbital pairs.

The remaining excited electronic states of **1** shown in Table 3 are placed in an energy range of 8.44−13.11 eV above the ground state. All these states arise from double excitations relative to the dominant configuration (eq 1) of the ground state. The electronic spectrum of **1** is not known experimentally. However, the dimethylated and bis(trifluoromethylated) compounds have in solution a UV absorption maximum at 335 nm

**TABLE 4: Weight of the Most Important Configurations in the MRD-CI/BS1 Wave Function ($\omega$, %) for the Low-Lying Electronic States of Dioxirane**

| | orbital occupation nos. | | | | | | $\omega$ | |
|---|---|---|---|---|---|---|---|---|
| state | $5a_1$ | $6a_1$ | $3b_2$ | $2b_1$ | $1a_2$ | $4b_2$ | I[a] | II[b] |
| $1^1A_1(4\pi)$ | 2 | 2 | 2 | 2 | 2 | 0 | 87.80 | |
| | 2 | 0 | 2 | 2 | 2 | 2 | 0.43 | |
| $1^3B_1(3\pi)$ | 2 | 2 | 2 | 2 | 1 | 1 | 87.97 | 60.86 |
| | 2 | 1 | 2 | 1 | 2 | 2 | 0.56 | 25.24 |
| $1^1B_1(3\pi)$ | 2 | 2 | 2 | 2 | 1 | 1 | 87.07 | 48.88 |
| | 2 | 1 | 2 | 1 | 2 | 2 | 1.30 | 34.86 |
| $1^3A_2(3\pi)$ | 2 | 2 | 2 | 1 | 2 | 1 | 85.97 | 72.38 |
| | 2 | 1 | 2 | 2 | 1 | 2 | 1.22 | 13.77 |
| $1^1A_2(3\pi)$ | 2 | 2 | 2 | 1 | 2 | 1 | 82.77 | 63.04 |
| | 2 | 1 | 2 | 2 | 1 | 2 | 3.52 | 21.47 |
| $1^3B_2(4\pi)$ | 2 | 2 | 2 | 1 | 1 | 2 | | 90.47 |
| | 2 | 1 | 2 | 2 | 2 | 1 | 75.90 | |
| | 1 | 2 | 2 | 2 | 2 | 1 | 13.60 | |
| $2^1A_1(3\pi)$[c] | 2 | 2 | 2 | 2 | 0 | 2 | 73.74 | 29.45 |
| | 2 | 2 | 2 | 0 | 2 | 2 | 13.49 | 60.28 |
| $2^3B_2(2\pi)$ | 2 | 2 | 2 | 1 | 1 | 2 | 90.39 | |
| | 2 | 1 | 2 | 2 | 2 | 1 | | 81.75 |
| $1^1B_2(4\pi)$ | 2 | 1 | 2 | 2 | 2 | 1 | 80.14 | 72.90 |
| | 1 | 2 | 2 | 2 | 2 | 1 | 2.90 | |
| $2^3B_1(3\pi)$ | 2 | 2 | 2 | 2 | 1 | 1 | 1.13 | 42.23 |
| | 2 | 2 | 2 | 1 | 1 | 2 | 85.69 | 11.81 |
| | 2 | 1 | 2 | 1 | 2 | 2 | | 21.24 |
| | 1 | 2 | 2 | 1 | 2 | 2 | | 11.27 |
| $2^3A_2(3\pi)$ | 2 | 2 | 1 | 1 | 2 | 2 | 9.91 | 25.22 |
| | 2 | 2 | 2 | 1 | 2 | 1 | | 29.78 |
| | 2 | 1 | 2 | 2 | 1 | 2 | 65.36 | 27.25 |
| $2^1B_1(3\pi)$ | 2 | 2 | 1 | 2 | 1 | 2 | 83.19 | 23.96 |
| | 2 | 2 | 2 | 2 | 1 | 1 | | 24.98 |
| | 2 | 1 | 2 | 1 | 2 | 2 | | 18.51 |
| | 1 | 2 | 2 | 1 | 2 | 2 | 2.26 | 20.16 |
| $2^1A_2(3\pi)$ | 2 | 2 | 1 | 1 | 2 | 2 | 47.36 | 38.52 |
| | 2 | 2 | 2 | 1 | 2 | 1 | | 22.99 |
| | 2 | 1 | 2 | 2 | 1 | 2 | 24.13 | 11.91 |
| | 1 | 2 | 2 | 2 | 1 | 2 | 10.47 | 14.50 |

[a] At the ground-state equilibrium geometry of dioxirane. [b] At the optimized geometry of each state. [c] The optimum geometry of this state is the ground state of dioxymethane, $1^1A_1(2\pi)$.

**TABLE 5: Geometrical Parameters,[a] Electric Dipole Moments ($\mu$, D),[b] Zero-Point Vibrational Energies (ZPVE, kcal/mol),[c] and Adiabatic Excitation Energies ($T_e$, eV),[d] of the Low-Lying Excited States of Dioxirane**

| state | $R$(CO) | $R$(CH) | ∠OCO | ∠HCH | $\mu$ | ZPVE | $T_e$ |
|---|---|---|---|---|---|---|---|
| $2^1A_2(2\pi)$[e] | 1.361 | 1.101 | 120.1 | 107.4 | 2.12 | 18.3 | 0.31 (0.00) |
| $1^3B_2(2\pi)$ | 1.386 | 1.093 | 115.8 | 108.1 | 2.09 | 18.6 | 0.47 (0.16) |
| $1^3A_2(3\pi)$ | 1.386 | 1.105 | 109.9 | 109.9 | 2.40 | 19.3 | 0.61 (0.30) |
| $1^1A_2(3\pi)$ | 1.389 | 1.104 | 110.8 | 108.8 | 2.30 | 19.9 | 0.74 (0.43) |
| $1^3B_1(3\pi)$ | 1.407 | 1.087 | 106.3 | 109.8 | 2.18 | 19.5 | 0.81 (0.50) |
| $1^1B_1(3\pi)$ | 1.407 | 1.086 | 109.6 | 109.4 | 2.12 | 19.5 | 1.04 (0.73) |
| $2^3B_2(4\pi)$ | 1.421 | 1.090 | 107.3 | 110.4 | 2.04 | | 1.21 (0.90) |
| $2^3B_1(3\pi)$ | 1.409 | 1.111 | 116.3 | 113.0 | 2.32 | | 3.62 (3.31) |
| $2^1A_2(3\pi)$ | 1.415 | 1.086 | 113.5 | 113.6 | 2.56 | | 3.65 (3.34) |
| $2^3A_2(3\pi)$ | 1.404 | 1.091 | 113.6 | 114.0 | 1.99 | | 3.87 (3.56) |
| $1^1B_2(4\pi)$ | 1.422 | 1.084 | 109.2 | 110.3 | 2.43 | | 4.12 (3.81) |
| $2^1B_1(3\pi)$ | 1.464 | 1.100 | 114.6 | 117.0 | 2.44 | | 4.42 (4.11) |

[a] Optimized at the MRD-CI/BS1 level; $C_{2v}$ symmetry, with distances in angstroms and angles in deg. [b] Calculated at the MRD-CI/BS2 level. [c] Obtained from CASSCF(6,4)/BS1 harmonic vibrational frequencies scaled by 0.8929. [d] Calculated at the MRD-CI+Q/BS2 level. The adiabatic excitation energies from the ground state of dioxymethane are given in parentheses. [e] This state is the ground state of dioxymethane, $1^1A_1(2\pi)$.

(3.70 eV)[5a,39] and 306 nm (4.05 eV),[5b] respectively, which can be related to the dipole-allowed vertical transition to the $1^1B_1(3\pi)$ state described above.

Within $C_{2v}$ molecular symmetry constraints, the optimum geometries of the above 12 electronic excited states of **1** were calculated at the MRD-CI/BS1 level. The most relevant geometrical parameters of the optimized structures are given in Table 5, along with the dipole moments calculated at the MRD-CI/BS2 level. Analytical harmonic vibrational frequencies were calculated at the CASSCF(6,4)/BS1 level for the lowest state of each symmetry and multiplicity. Excluding the $1^1B_2(4\pi)$ state, which showed an imaginary frequency ($\nu = 4473i$ cm$^{-1}$), in all cases the harmonic vibrational analysis of these states indicated that the optimized structure was a true potential energy minimum (no imaginary frequencies). The ZPVE calculated from these vibrational frequencies scaled by 0.8929 are also included in Table 5. The energies of the 12 excited states relative to the ground state of **1**, namely the adiabatic excitation energies, computed at the MRD-CI+Q/BS2 level are shown in last column of Table 5. Detailed information about the MRD-CI wave functions calculated for each excited state is given in last column of Table 4.

First of all, we note that all calculated excited states show an optimum ∠OCO ranging from 106.3 to 120.1°. The OO bond in these states is thus fully broken, so it is more appropriate to consider them as excited electronic states of **2** rather than of **1**. For the purpose to facilitate possible comparisons, the adiabatic excitation energies relative to ground state of **2** are also given in parentheses in last column of Table 5. As pointed out in section I, no previous adiabatic excitation energies have been reported for **2**, except the values of 0.50 and 1.15 eV, calculated at the QCISD(T)/6-31G(d) level using MP2/6-31G(d) optimized geometries, reported by Bach and co-workers[15b] for two excited states, corresponding to a $3\pi$- and a $4\pi$-electron singlets. Since the symmetry of these excited states was not specified, a comparison with the present results is not possible.

A comparison between Tables 3 and 5 reveals that the energy ordering found for the vertical excited states of **1** changes dramatically upon relaxation of the geometrical parameters to the corresponding optimum values. For instance, the first vertical excited state of **1** is predicted to be a $3\pi$-electron triplet of $B_1$ symmetry, while a $2\pi$-electron triplet of $B_2$ symmetry comes out to be the first adiabatic excited state of **2**. In addition, the energy ordering calculated for the lower $^3B_2(4\pi)$ and $^3B_2(2\pi)$ states is reversed in passing from the ground-state equilibrium geometry of **1** to the optimum geometry of each state. This result indicates that when the geometry is relaxed from the Frank Condon to the adiabatic region, the PESs of these electronic states cross one another. This feature was explored by computing the adiabatic PECs for the $^3B_2(4\pi)$ and $^3B_2(2\pi)$ states as function of ∠OCO. The MRD-CI/BS1 energy was used in these computations. For both states ∠OCO was varied and all other parameters were optimized at each fixed value of ∠OCO keeping $C_{2v}$ symmetry. An intersection between the two PECs was found at some molecular geometry close to ∠OCO = 92.5°.[40] A comparison between the equilibrium geometries predicted for the $^3B_2(2\pi)$ and $^3B_2(4\pi)$ states shows that ∠OCO is 8.5° wider in the first structure. This result is in accordance with the double occupation of the OO-antibonding $4b_2$ MO in $^3B_2(2\pi)$, as compared with the single occupation of this orbital in $^3B_2(4\pi)$.

Another interesting result is that the energy ordering of the $1^3A_2(3\pi)$ and $1^3B_1(3\pi)$ states, as well as that of the $1^1A_2(3\pi)$ and $1^1B_1(3\pi)$ states, is reversed in passing from the equilibrium geometry calculated for the ground state of **1** to the optimum geometries of these states. Thus, at their equilibrium geometries the $1^3A_2(3\pi)$ and $1^1A_2(3\pi)$ states lie below the energies of the $1^3B_1(3\pi)$ and $1^1B_1(3\pi)$ states. This relative energy ordering is just opposite of the calculated ordering for these states at the equilibrium geometry of ground-state **1** (see Table 3). These features suggest possible $1^3A_2(3\pi)/1^3B_1(3\pi)$ and $1^1A_2(3\pi)/1^1B_1(3\pi)$ PES intersections. Both surface intersections were investigated by computing at the MRD-CI/BS1 level the corresponding adiabatic PECs as function of ∠OCO angle keeping $C_{2v}$ symmetry and optimizing all other geometric parameters. A $1^3A_2(3\pi)/1^3B_1(3\pi)$ intersection point was found at some molecular geometry close to ∠OCO = 95.0°.[41] It is worthy of mention that such an intersection point is just one arbitrary point on the intersection seam between the PESs of these states and not necessarily anywhere near the minimum energy crossing point. Analogously, the PECS calculated for the $1^1A_2(3\pi)$ and $1^1B_1(3\pi)$ states showed an intersection point near ∠OCO = 87.5°.[42] Similar intersections have also been found between the $1^1A_2$ and $1^1B_1$ states of the isoelectronic ozone molecule.[27,43,44] The remarkable finding that in the adiabatic region the $1^3A_2$ and $1^1A_2$ states of **2** are lower in energy than the $1^3B_1(3\pi)$ and $1^1B_1(3\pi)$ states may be explained by analyzing how the MRD-CI wave function of these states changes in passing from the Franck−Condon to the adiabatic region. As shown in Table 4, at the ground-state equilibrium geometry of **1** the wave function of both the $1^3B_1(3\pi)$ and $1^1B_1(3\pi)$ states is dominated by a configuration (eq 2) involving a single excitation from the $\pi$ OO-antibonding $1a_2$ MO to the $\sigma$ OO-antibonding $4b_2$ orbital, whereas the wave function of both the $1^3A_2(3\pi)$ and $1^1A_2(3\pi)$ states is dominated by a configuration (eq 3) involving a single excitation from the $\pi$ OO-bonding $2b_1$ MO to the $4b_2$ orbital. Since the latter excitation is likely to be of higher energy than the former, it follows that in the Franck−Condon region the triplet and singlet states of $B_1$ symmetry are expected to lie below the triplet and singlet states of $A_2$ symmetry. In the adiabatic region the wave functions of these $B_1$ and $A_2$ states still are dominated by the above singly excited configurations, but a second doubly excited configuration appears to have an important weight. This doubly excited configuration involves a single excitation from the $\sigma$ OO-bonding $6a_1$ MO to the $\sigma$ OO-antibonding $4b_2$ orbital together with one of the two

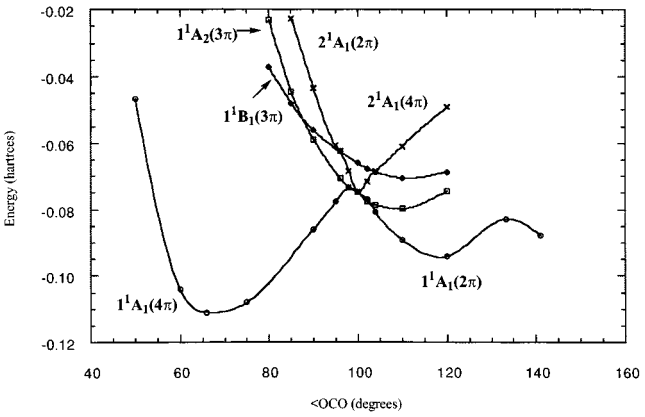


**Figure 1.** Plots of total energy of the lower $^1A_1(4\pi)$, $^1B_1(3\pi)$, $^1A_2(3\pi)$, and $^1A_1(2\pi)$ states of dioxane and dioxymethane as a function of the OCO angle. The total electronic energies are relative to −189.00 hartree.

**TABLE 6: Geometrical Parameters[a] and Total Energies (*E*, hartree)[b] Calculated for the Minimum Energy Crossing Points between the Potential Energy Surfaces of the Low-Lying Singlet States of Dioxirane**

| states | *R*(CO) | *R*(CH) | ∠OCO | ∠HCH | *E* |
|---|---|---|---|---|---|
| $1^1A_2(3\pi)/1^1B_1(3\pi)$ | 1.414 | 1.078 | 91.0 | 111.4 | −189.060 65/ −189.056 96 (2.3) |
| $1^1B_1(3\pi)/^1A_1(2\pi)$ | 1.395 | 1.083 | 96.7 | 111.0 | −189.062 79/ −189.064 56 (1.1) |
| $1^1A_2(3\pi)/^1A_1(4\pi)$ | 1.381 | 1.085 | 101.4 | 110.8 | −189.076 46/ −189.072 63 (2.4) |
| $1^1B_1(3\pi)/^1A_1(4\pi)$ | 1.388 | 1.084 | 104.6 | 110.6 | −189.068 65/ −189.067 27 (0.9) |

[a] Optimized at the CASSCF(6,4)/BS1 level; $C_{2v}$ symmetry, with distances in angstroms and angles deg. [b] Calculated at the MRD-CI+Q/BS1 level. The energy differences between the two crossing states are given in parentheses in kcal/mol.

aforementioned single excitations, namely $2b_1 \rightarrow 4b_2$ for the $B_1$ states and $1a_2 \rightarrow 4b_2$ for the $A_2$ states. On the basis that the former single excitation is likely to be of higher energy than the latter, it is easily understood why in the adiabatic region the $1^3A_2(3\pi)$ and $1^1A_2(3\pi)$ states of **1** are predicted to be lower in energy than the $1^3B_1(3\pi)$ and $1^1B_1(3\pi)$ states.

In connection with the observed photochemical decomposition of substituted dioxiranes,[45−47] it is worthy to examine all together the PECs calculated for the first four singlet states, namely $^1A_1(4\pi)$, $1^1B_1(3\pi)$, $1^1A_2(3\pi)$, and $^1A_1(2\pi)$, shown in Figure 1. It is readily seen from inspection of Figure 1 that several intersections between the different PECs occur in an ∠OCO range of 90−110°. Besides the $^1A_1(4\pi)/^1A_1(2\pi)$ and $1^1A_2(3\pi)/1^1B_1(3\pi)$ PECs intersections discussed above, we note that the $1^1B_1(3\pi)$ PEC intersects the $^1A_1(2\pi)$ and $^1A_1(4\pi)$ PECs at ∠OCO near 96 and 104°, respectively. Moreover, the $1^1A_2(3\pi)$ PEC intersects the $^1A_1(4\pi)$ PEC near ∠OCO = 100°. The region corresponding to an ∠OCO ranging from 90 to 110° was further investigated by searching at the CASSCF(6,4)/BS1 level the minimum energy points on the $1^1A_2(3\pi)/1^1B_1(3\pi)$, $1^1B_1(3\pi)/^1A_1(2\pi)$, $1^1A_2(3\pi)/^1A_1(4\pi)$, and $1^1B_1(3\pi)/^1A_1(4\pi)$ intersection seams using the constrained optimization algorithm of Ragazos and co-workers[48] implemented in Gaussian 94 program package. The geometrical parameters of the CASSCF(6,4)/BS1 optimized structures for the minimum energy points on the aforementioned intersection seams are given in Table 6 along with the total energies of the crossing states calculated at the MRD-CI/BS1 level. As expected, while at the CASSCF(6,4)/BS1 level the energy difference between the two crossing states was calculated to be less than 0.1 kcal/mol for each optimized minimum energy crossing point, this energy difference comes out to be somehow larger (i.e., in the 0.9−2.4 kcal/mol range) at the MRD-CI+Q/BS1 level. The existence of minimum energy intersection points between the low-lying singlet states of **1** suggest that, in addition to the thermal ring opening of **1** to give **2** taking place on the ground-state PES, the ring opening of **1** into **2** may occur photochemically via a mechanism involving a vertical electronic excitation to either the $1^1B_1(3\pi)$ or $1^1A_2(3\pi)$ states and subsequent radiationless decay to the ground state of **2** through minimum energy intersection points on the PESs of the appropriate states. These photochemical pathways might account for the observed photochemical decomposition of substituted dioxiranes.[45−47]

**TABLE 7: Dissociation Energies ($D_e$, kcal/mol) of the Five Lower Electronic States of Dixoymethane[a]**

| dissociation channel | $D_e$ |
|---|---|
| $H_2CO_2$ ($1^1A_1$) → $CO_2$ ($^1\Sigma_g^+$) + $H_2$ ($^1\Sigma_g^+$) | −99.7 (−105.2)[b] |
| $H_2CO_2$ ($1^3B_2$) → $CO_2$ ($^3B_2$) + $H_2$ ($^1\Sigma_g^+$) | 8.1 |
| $H_2CO_2$ ($1^3A_2$) → $CO_2$ ($^3A_2$) + $H_2$ ($^1\Sigma_g^+$) | 17.9 |
| $H_2CO_2$ ($1^1A_2$) → $CO_2$ ($^1A_2$) + $H_2$ ($^1\Sigma_g^+$) | 20.2 |
| $H_2CO_2$ ($1^3B_1$) → $CO_2$ ($^3B_1$) + $H_2$ ($^1\Sigma_g^+$) | 78.5 |

[a] Calculated at the MRD-CI+Q/BS2 level. Energies of the dissociation products (hartrees): −188.19734 ($CO_2$ ($^1\Sigma_g^+$)), −188.01954 ($CO_2$ ($^3B_2$)), −187.99876 ($CO_2$ ($^3A_2$)), −187.99036 ($CO_2$ ($^1A_2$)), −187.89488 ($CO_2$ ($^3B_1$)), and −1.16567 ($H_2$ ($^1\Sigma_g^+$)). [b] ZPVE corrected value. ZPVE of the dissociation products are obtained from CASSCF/BS1 harmonic vibrational frequencies scaled by 0.8929 (kcal/mol): 6.6 ($CO_2$ ($^1\Sigma_g^+$)) and 6.2 ($H_2$ ($^1\Sigma_g^+$)).

**Dissociation of Dioxymethane into $CO_2$ and $H_2$.** Table 7 summarizes the MRD-CI+Q/BS2 calculated dissociation energies of the lower singlet and triplet states of **2** for their dissociation into ground-state $H_2$ plus $CO_2$ in its ground or low-lying excited states. As seen in Table 7, the dissociation of ground-state **2** into the ground states of $CO_2$ and $H_2$ is predicted to be exothermic by 105.2 kcal/mol at the MRD-CI+Q level with the BS2 basis plus ZPVE correction. If $C_{2v}$ symmetry is maintained, a transition structure (**TS2**) interconnecting **2** with the dissociation products in their ground states was located on the ground-state PES of **2** at the MRD-CI/BS1 level. The saddle point nature of **TS2** was confirmed by computing the harmonic vibrational frequencies of this structure after its geometry reoptimization at the CASSCF(6,4)/BS1 level. The geometrical parameters, electric dipole moment, ZPVE, and total energy of **TS2** are compared in Table 8 with those calculated at the same level of theory for the ground state of **2**. The calculated geometrical parameters of **TS2** are in fairly good agreement with the only earlier MCSCF results of Karlström and co-workers,[14] namely *R*(CO) = 1.240 Å, *R*(CH) = 1.210 Å, *R*(HH) = 1.240 Å, and ∠OCO = 139.0. The $C_{2v}$ symmetry found for **TS2** indicates that the dissociation of ground-state **2** into $CO_2$ and $H_2$ takes place via a concerted mechanism involving the synchronous breaking of the two CH bonds along with the formation of the HH bond. According to Table 8, a potential energy barrier of 5.8 kcal/mol is predicted for this dissociation at the MRD-CI+Q/BS2 level. This energy barrier can be compared with the earlier reported value of 28.3 kcal/mol computed at the MCSCF level by Karlström and co-workers, which is about five times higher.[14] On the basis of the reasonable agreement found between the geometrical parameters calculated for **2** and **TS2** at the MRD-CI and MCSCF levels of theory, the origin of the much larger energy barrier predicted by the MCSCF calculations is unclear. However, this discrepancy points out the importance of including dynamical electron correlation in computing the energetics for the dissociation of ground-state **2** into $CO_2$ and $H_2$. From the ZPVE corrected

**TABLE 8: Geometrical Parameters,[a] Electric Dipole Moments ($\mu$, D),[b] Zero-Point Vibrational Energies (ZPVE, kcal/mol),[c] Total Energies ($E$, hartree),[d] and Relative Energies ($E_{rel}$, kcal/mol),[d,e] Calculated for the Ground State of Dioxymethane (2) and the Transition Structure (TS2) for its Dissociation into the Ground States of $CO_2$ and $H_2$**

| structure | $R$(CO) | $R$(CH) | $R$(HH) | ∠OCO | ∠HCH | $\mu$ | ZPVE | $E$ | $E_{rel}$ |
|---|---|---|---|---|---|---|---|---|---|
| **2** | 1.361 | 1.101 | 1.775 | 120.1 | 107.4 | 2.12 | 18.3 | −189.204 10 | 0.0 |
| **TS2** | 1.290 | 1.135 | 1.333 | 133.4 | 71.9 | 3.21 | 15.7 | −189.194 78 | 5.8 (3.2) |

[a] Optimized at the MRD-CI/BS1 level; $C_{2v}$ symmetry, with distances in angstroms and angles in deg. [b] Calculated at the MRD-CI+Q/BS2 level. [c] Obtained from CASSCF(6,4)/BS1 harmonic vibrational frequencies scaled by 0.8929. [d] MRD-CI+Q/BS2 energies at the MRD-CI/BS1 optimized geometries. [e] ZPVE corrected values are given in parentheses.

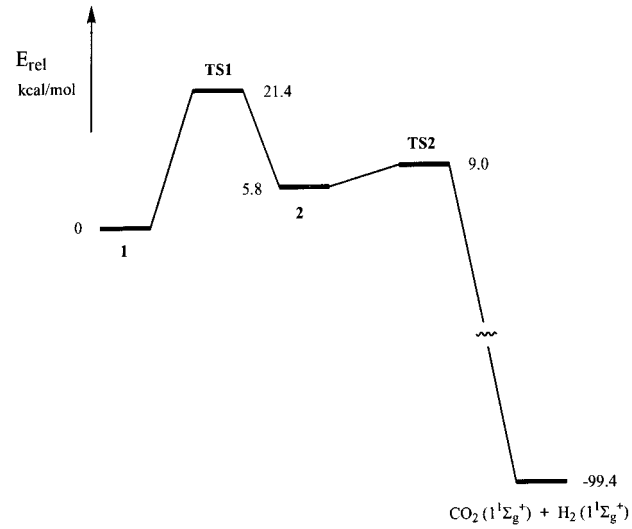


**Figure 2.** Schematic potential energy profile showing the two-step process required for the ground-state dissociation of dioxirane into $CO_2$ and $H_2$. Energy values obtained from the ZPVE-corrected MRDCI+Q/BS2 energies are relative to that of dioxirane.

MRD-CI+Q/BS2 energies of Table 8 a 0 K activation energy of 3.2 kcal/mol is predicted. It is worthy noting this low energy of activation is consistent with the large exothermicity of 105.2 kcal/mol predicted for the dissociation of ground-state **2**.[49] Combining the MRD-CI+Q/BS2+ZPVE relative energies of Tables 2, 7, and 8 allows us to construct the schematic potential energy profile depicted in Figure 2, which summarizes the two-step process required for the ground-state dissociation of **1** into $CO_2$ and $H_2$. From this energy profile we conclude that **TS1** is the rate-determinant transition structure for the overall process, which involves an activation energy of 21.4 kcal/mol and a reaction energy of −99.4 kcal/mol at 0 K.

Regarding the first four excited states of **2**, Table 7 shows that at the MRD-CI+Q/BS2 level the dissociation into ground-state $H_2$ and the corresponding excited state of $CO_2$ is found to be endothermic for all these states, the predicted endothermicity ranging from 8.1 to 78.5 kcal/mol. This result can be rationalized by comparing Tables 1 and 5. Thus for $CO_2$ the $1^3B_2$, $1^3A_2$, and $1^1A_2$ excited states lie high in energy above the ground state (i.e., 111.6−129.8 kcal), while in the case of **2** these states lie much lower in energy (i.e., 10.8−17.1 kcal/mol). Therefore, the larger energy gap between the ground and excited states found for $CO_2$, as compared with **2**, does not compensate the 99.7 kcal/mol energy lowering accompanying the dissociation of ground-state **2**.

## V. Summary and Conclusions

In this paper, we have investigated the low-lying electronic states of dioxirane, their ring opening to dioxymethane, and the dissociation of dioxymethane into $CO_2$ and $H_2$ by means of CASSCF and MRD-CI+Q quantum chemistry calculations. The following points emerge from this investigation:

(1) The ground state of dioxirane is a singlet with $4\pi$ electrons, $1^1A_1(4\pi)$, while the ground state of dioxymethane is a $2\pi$-electron singlet, $1^1A_1(2\pi)$, lying 5.8 kcal/mol above the ground state of dioxirane. The ground-state ring opening of dioxirane to dioxymethane takes place via a transition state approximately corresponding to the crossing between the lower $^1A_1(4\pi)$ and $^1A_1(2\pi)$ states of both molecules. A 0 K activation energy of 21.4 kcal/mol is predicted for this thermal ring opening.

(2) Dioxirane has 12 excited states with vertical excitation energies ranging from 3.07 to 13.11 eV. At the ground-state geometry, the lowest excited state is a $3\pi$-electron triplet of $B_1$ symmetry. A vertical excitation energy of 4.23 eV is found for the corresponding singlet state, which is predicted to be the lowest excited singlet state of dioxirane. The vertical transition to the latter state is dipole-allowed and can be related to the observed UV absorption of the dimethylated and bis(trifluoromethylated) dioxiranes maxima at 3.70 and 4.05 eV, respectively.

(3) The adiabatic excitation energies of the above 12 states range from 0.47 to 4.42 eV. The optimized geometry of these states show an ∠OCO ranging from 106.3 to 120.1°. Consequently, these should be considered as excited electronic states of dioxymethane rather than of dioxirane. A $2\pi$-electron triplet of $B_2$ symmetry lying only 0.16 eV above the ground state of dioxymethane is predicted to be the first excited state of this species. The remaining excited states of dioxymethane are located in an energy range of 0.30−4.11 eV.

(4) The energy ordering found for the excited states of dioxirane changes dramatically upon relaxation of the molecular geometries. Minimum energy points of the intersection seam between the $1^1A_2(3\pi)/1^1B_1(3\pi)$, $1^1B_1(3\pi)/^1A_1(2\pi)$, $1^1A_2(3\pi)/^1A_1(4\pi)$, and $1^1B_1(3\pi)/^1A_1(4\pi)$ PESs were located in an ∠OCO range of 91.0−104.6°. These findings suggest that, in addition to the thermal ring opening of ground-state dioxirane to dioxymethane, this isomerization may occur photochemically via a mechanism involving vertical electronic excitation to either the $1^1B_1(3\pi)$ or $1^1A_2(3\pi)$ states and subsequent radiationless decay to the ground state of **2** through minimum energy intersection points on the PESs of the appropriate states. These photochemical pathways might account for the observed photochemical decomposition of substituted dioxiranes.

(5) The dissociation of ground-state dioxymethane into the ground states of $CO_2$ and $H_2$ is predicted to be exothermic by 105.2 kcal/mol with an activation energy of 3.2 kcal/mol at 0 K. The dissociation takes place via a $C_{2v}$ transition structure involving the synchronous breaking of the two CH bonds along with formation of the HH bond. On the contrary, the dissociations of the first four excited states of dioxymethane, namely $1^3B_2(2\pi)$, $1^3A_2(3\pi)$, $1^1A_2(3\pi)$, and $1^3B_1(3\pi)$, into ground-state $H_2$ and the corresponding excited state of $CO_2$ are all predicted to be endothermic, with endothermicities ranging from 8.1 to 78.5 kcal/mol.

**Acknowledgment.** This paper is dedicated to Professor Fransesc Trull, deceased in June 1997. The work was supported by the Dirección General de Investigación Científica y Técnica (DGICYT Grants PB95-0278-C01 and PB95-0278-C02). The computations were performed on two IBM RS6000 workstations at the CID of CSIC, on the CONVEX C-3480 at the CEPBA and on the IBM SP2 at the CESCA. The authors also wish to thank Professor Sigrid D. Peyerimhoff and Dr. Michael W. Schmidt for providing a copy of the MRD-CI and GAMESS codes, respectively.

## References and Notes

(1) Bailey, P. S. *Ozonation in Organic Chemistry*; Academic Press: New York, 1978, 1982; Vols. 1 and 2.

(2) For reviews see: (a) Sander, W. *Angew. Chem, Int. Ed. Engl.* **1990**, *29*, 344. (b) Bunnelle, W. *Chem. Rev.* **1991**, *91*, 335.

(3) (a) Lovas, F. J.; Suenram, R. D. *Chem. Phys. Lett.* **1977**, *51*, 453. (b) Suenram, R. D.; Lovas, F. J. *J. Am. Chem. Soc.* **1978**, *100*, 5117.

(4) Martinez, R. I.; Huie, R. E.; Herron, J. T. *Chem. Phys. Lett.* **1977**, *51*, 457.

(5) (a) Murray, R. W.; Jeyaraman, R. *J. Org. Chem.* **1985**, *50*, 2847. (b) Mello, R.; Fiorentino, M.; Sciacovelli, O.; Curci, R. *J. Org. Chem.* **1988**, *53*, 3890. (c) Bucher, G.; Sander, W. *Chem. Ber.* **1992**, *12*, 1851. (d) Russo, A.; DesMarteau, D. D. *Angew. Chem., Int. Ed. Engl.* **1993**, *32*, 905.

(6) Criegee, R. *Angew. Chem., Int. Ed. Engl.* **1975**, *14*, 745.

(7) (a) Mimoun, H. *Angew. Chem., Int. Ed. Engl.* **1982**, *21*, 734. (b) Adam, W.; Curci, R.; Edwards, J. O. *Acc. Chem. Res.* **1989**, *22*, 205.

(8) (a) Murray, R. W.; Ramachandran, V. *Photochem. Photobiol.* **1979**, *30*, 187. (b) Murray, R. W. *Chem. Rev.* **1989**, 89, 1187.

(9) Dix, T. A.; Benkovic, S. *Acc. Chem. Res.* **1988**, *21*, 101.

(10) (a) Atkinson, R.; Carter, W. P. L. *Chem. Rev.* **1984**, *84*, 437. (b) Atkinson, R.; Lloyd, A. *J. Phys. Chem. Ref. Data* **1984**, *13*, 315.

(11) Curci, R. In *Advances in Oxygenated Processes*; Baumstark, A. L., Ed.; JAI Press: Greenwitch, CT, 1990; p 1.

(12) (a) Wadt, W. R.; Goddard, W. A., III. *J. Am. Chem. Soc.* **1975**, *97*, 3004. (b) Harding, L. B.; Goodard, W. A., III. *J. Am. Chem. Soc.* **1978**, *100*, 7180.

(13) Cremer, D.; Schmidt, T.; Gauss, J.; Radhakrisnan, T. P. *Angew. Chem., Int. Ed. Engl.* **1988**, *27*, 427.

(14) Karlström, G.; Engström, S.; Jönsson, B. *Chem. Phys. Lett.* **1979**, *67*, 343.

(15) (a) Bach, R. D.; Owensby, A. L.; Andrés, J. L.; Schlegel, H. B. *J. Am. Chem. Soc.* **1991**, *113*, 7031. (b) Bach, R. D.; Andrés, J. L.; Owensby, A. L.; Schlegel, H. B.; McDouall, J. J. W. *J. Am. Chem. Soc.* **1992**, *114*, 7207.

(16) Cantos, M.; Merchan, M.; Tomas-Vert, F.; Roos, B. O. *Chem. Phys. Lett.* **1994**, *229*, 181.

(17) (a) Herron, J. T.; Huie, R. E. *J. Am. Chem. Soc.* **1977**, *99*, 5430. (b) Martinez, R. I.; Herron, J. T. *J. Phys. Chem.* **1987**, *91*, 946. (c) Martinez, R. I.; Herron, J. T. *J. Phys. Chem.* **1988**, *92*, 4644.

(18) (a) Cramer, D. *J. Am. Chem. Soc.* **1979**, *101*, 7189. (b) Francisco, J. S.; Williams, I. H. *Chem. Phys.* **1985**, *95*, 71. (c) Gauss, J.; Cremer, D. *Chem. Phys. Lett.* **1987**, *133*, 420. (d) Gauss, J.; Cremer, D. *Chem. Phys. Lett.* **1989**, *163*, 549. (c) Cremer, D.; Schmidt, T.; Sander, W.; Bischof, P. *J. Org. Chem.* **1989**, *54*, 2515. (f) Cremer, D.; Gauss, J.; Kraka, E.; Stanton, J. F. *Chem. Phys. Lett.* **1993**, *209*, 547. (g) Kim, S.-J.; Schaefer, H. F., III; Kraka, E.; Cremer, D. *Mol. Phys.* **1996**, *88*, 93. (h) Anglada, J. M.; Bofill, J. M.; Olivella, S.; Sole, A. *J. Am. Chem. Soc.* **1996**, *118*, 4636.

(19) Cimiraglia, R.; Ha, T.-K.; Meyer, R.; Günthard, H. H. *Chem. Phys. Lett.* **1982**, *66*, 209.

(20) (a) Buenker, R. J.; Peyerimhoff, S. D. *Theor. Chim. Acta* **1974**, *35*, 33. (b) Buenker, R. J.; Peyerimhoff, S. D. *Theor. Chim. Acta* **1975**, *39*, 217. (c) Buenker, R. J.; Peyerimhoff, S. D.; Butscher, W. *Mol. Phys.* **1978**, *35*, 771. (d) Buenker, R. J.; Peyerimhoff, S. D. In *New Horizons of Quantum Chemistry*; Lowdin, P. O., Pullman, B., Eds.; D. Reidel: Dordrecht, The Netherlands, 1983; p 183. (e) Buenker, R. J.; Philips, R. A. *J. Mol. Struct. THEOCHEM* **1985**, *123*, 291.

(21) Davidson, E. R. In *New Horizons of Quantum Chemistry*; Lowdin, P. O., Pullman, B., Eds.; D. Reidel: Dordrecht, The Netherlands, 1983; p 17. (b) Langhoff, S. R.; Davidson, E. R. *Int. J. Quantum Chem.* **1974**, *8*, 61.

(22) (a) Buenker, R. J.; Peyerimhoff, S. D.; Bruna, P. J. In *Computational Theoretical Organic Chemistry, NATO ASI*; Csizmadia, I. G., Daudel, R., Eds.; D. Reidel: Dordrecht, The Netherlands, 1981; p 55. (b) Burton, P. G.; Buenker, R. J.; Bruna, P. J.; Peyerimhoff, S. D. *Chem. Phys. Lett.* **1983**, *95*, 379.

(23) Hariharan, P. C.; Pople, J. A. *Theor. Chim. Acta* **1973**, *28*, 213.

(24) Huzinaga, S. *J. Chem. Phys.* **1965**, *42*, 1293.

(25) Dunnig, T. H. *J. Chem. Phys.* **1970**, *53*, 2823.

(26) Dunnig, T. H.; Hay, P. J. In *Modern Theoretical Chemistry*; Schaefer, H. F., Ed.; Plenum: New York, 1977; Vol. 3, p 1.

(27) Banichevich, A.; Peyerimhoff, S. D. *Chem. Phys.* **1993**, 174, 93.

(28) Dunnig, T. H. *J. Chem. Phys.* **1989**, *90*, 1007.

(29) Bauschlicher, C. W., Jr. *J. Chem. Phys.* **1986**, *85*, 6510.

(30) Spieldfiedel, A.; Feautrier, N.; Cossart-Magos, C.; Werner, H.-J.; Botschwina, P. *J. Chem. Phys.* **1992**, *97*, 8382.

(31) Anglada, J. M.; Bofill, J. M. *Theor. Chim. Acta* **1995**, *92*, 369.

(32) Bofill, J. M. *J. Comput. Chem.* **1994**, *15*, 1.

(33) For a review, see: Roos, B. O. *Adv. Chem. Phys.* **1987**, *69*, 399.

(34) (a) Pulay, P. In *Modern Theoretical Chemistry*; Schaefer, H. F., Ed.; Plenum: New York, 1977; Vol. 4, p 153. (b) Pulay, P.; Fogarasi, G.; Pang, F.; Boggs, J. E. *J. Am. Chem. Soc.* **1979**, *101*, 2550.

(35) Curtiss, L. A.; Raghavachari, K.; Trucks, G. W.; Pople, J. A. *J. Chem. Phys.* **1991**, *94*, 7221.

(36) Schmidt, M. W.; Baldrige, K. K.; Boatz, J. A.; Jensen, J. H.; Koseki, S.; Gordon, M. S.; Nguyen, K. A.; Windus, T. L.; Elbert, S. T. Gamess. *QCPE Bull.* **1990**, *10*, 52.

(37) Frisch, M. J.; Trucks, G. W.; Schlegel, H. B.; Gill, P. M. W.; Johnson, B. G.; Robb, M. A.; Cheeseman, J. R.; Keitth, T. A.; Petersson, G. A.; Montgomery, J. A.; Raghavachari, K.; Al-Laham, M. A.; Zakrzewski, V. G.; Ortiz, J. V.; Foresman, J. B.; Cioslowski, J.; Stefanov, A.; Nanayakkara, A.; Challacombe, M.; Peng, C. Y.; Ayala, P. Y.; Chen, W.; Wong, M. W.; Andres, J. L.; Replogle, E. S.; Gomperts, R.; Martin, R. L.; Fox, D. J.; Binkley, J. S.; Defrees, D. J.; Baker, J.; Stewart, J. J. P.; Head-Gordon, M.; Gonzalez, C.; Pople, J. A. *GAUSSIAN 94*; Gaussian, Inc.: Pittsburgh, PA, 1995.

(38) MRD-CI+Q/BS2 energy in hartrees: −189.179 18.

(39) Adam, W.; Chan, Y.-Y.; Cremer, D.; Gauss, J.; Scheutzow, D.; Schindler, M. *J. Org. Chem.* **1987**, *52*, 2800.

(40) Optimized geometrical parameters for ∠OCO = 95.5°: $R$(CO) = 1.429 Å, $R$(CH) = 1.086 Å, and ∠HCH = 112.0°. MRD-CI+Q/BS1 energies in hartrees: −189.054 15 ($^3B_2(4\pi)$) and −189.053 89 ($^3B_2(2\pi)$).

(41) Optimized geometrical parameters for ∠OCO = 95.0°: $R$(CO) = 1.404 Å, $R$(CH) = 1.085 Å, and ∠HCH = 109.4°. MRD-CI+Q/BS1 energies in hartrees: −189.073 37 ($^3B_1(3\pi)$) and −189.074 31 ($^3A_2(3\pi)$).

(42) Optimized geometrical parameters for ∠OCO = 87.5°: $R$(CO) = 1.418 Å, $R$(CH) = 1.085 Å, and ∠HCH = 111.1°. MRD-CI+Q/BS1 energies in hartrees: −189.052 46 ($^1B_1(3\pi)$) and −189.051 77 ($^1A_2(3\pi)$).

(43) Braunstein, M.; Hay, P. J.; Martin, R. L.; Pack, R. T. *J. Chem. Phys.* **1991**, *95*, 8329.

(44) Banichevich, A.; Peyerimhoff, S. D.; Grein, F. *Chem.* Phys. **1993**, *178*, 155.

(45) Ganzer, G. A.; Sheridan, R. S.; Liu, M. T. H. *J. Am. Chem. Soc.* **1986**, *108*, 1517.

(46) (a) Sander, W. *J. Org. Chem.* **1988**, *53*, 121. (b) Sander, W. *J. Org. Chem.* **1988**, *53*, 2091. (c) Sander, W. *J. Org. Chem.* **1989**, *54*, 333.

(47) Adam, W.; Curci, R.; Gonzalez-Nuñez, M. E.; Mello, R. *J. Am. Chem. Soc.* **1991**, *113*, 7654.

(48) Ragazos, I. N.; Robb, M. A.; Bernardi, F.; Olivucci, M. *Chem. Phys. Lett.* **1992**, *197*, 217.

(49) Hammond, G. S. *J. Am. Chem. Soc.* **1955**, *77*, 334.